

Histopathologic studies of autopsy eyes with surgically closed macular holes showed that the holes were closed by glial cells, most likely Müller cells or astrocytes.^{22,32,33} The closed macular hole restored the physiologic foveal depression, but a small break can still remain in the ELM with reapproximation of the edges by the proliferation of cells filling the small gap.²⁶ The small break in ELM by SD-OCT has been considered to be the cause of the foveal hyper-reflective lesions.²⁶ The hyper-reflective lesion was observed to become smaller with increasing time.

Small breaks in the COST line may be related to the decreased signals behind the hyper-reflective lesion or a foveal displacement of proliferative glial cells resulting in the alteration of the COST line at the fovea. Ooto and associates³⁴ used an adaptive optics scanning laser ophthalmoscope to determine the cone photoreceptor density in patients with central serous chorioretinopathy and compared their findings with the microstructures determined by a commercially available SD-OCT. They found that the mean cone density in eyes with disrupted COST line was significantly lower than that in eyes with intact COST line, and the cone density in the foveal area was correlated with the BCVA. Each possibility is supported by the findings that the alteration of the COST line was closely related to the postoperative visual acuity. Eyes with larger preoperative macular holes were reported to be associated with poorer postoperative visual acuity.^{14,15,35} We determined the relationship of the apical diameter of the macular hole with the postoperative COST line. We found that the mean preoperative macular hole diameter was not significantly correlated with the integrity of the COST line, although the duration of symptoms was

significantly shorter in the eyes with COST+ than in eyes with COST-. This may be attributable to the smaller numbers of eyes with COST+ than with IS/OS+/ELM+.

The recovery of the IS/OS junction and ELM detected at 1 month was earlier than that of a distinct COST line, which was detected at 6 months. This difference could be explained by the difference in the recovery of the rods and cones, as shown after experimental retinal detachment in rhesus monkeys.³⁰ The regeneration of cone outer segments was slower than the rod outer segment even after 1 month, and it took 5 months to achieve equal length of photoreceptor outer segments without statistical difference from the control areas. We assume that the delayed regeneration of cone outer segments may cause a delay in the recovery of the COST line in a similar way.

This study has limitations in that it was a retrospective study without a control group. In addition, the number of patients in each group was small. Therefore, further studies with larger sample sizes are needed to confirm these results. Nevertheless, the results showed that the integrity of the COST line rather than the IS/OS junction and the ELM may be more useful clinically to indicate good photoreceptor restoration and higher-level visual recovery in patients with surgically closed macular holes.

In conclusion, BCVA improved after successful macular hole surgery in eyes that had a distinct COST line in the SD-OCT images. The COST line can be a critical finding accounting for good BCVA at the time of SD-OCT examination, but is not useful for predicting subsequent visual recovery, although the restoration of the foveal IS/OS junction and ELM was necessary to achieve COST line recovery.

THE AUTHORS INDICATE THAT NO GOVERNMENT OR NONGOVERNMENT FINANCIAL SUPPORT WAS INVOLVED IN THE WORK for this submission. The authors have no proprietary or commercial interest in any materials discussed in this article. Dr Inoue has received speaker support from Alcon Japan, Ltd; Santen Pharmaceutical Inc; HOYA Corp; and Kowa Pharmaceutical Co Ltd. Dr Hirakata has received speaker support from Alcon Japan, Ltd; Santen Pharmaceutical Inc; Novartis Pharma K.K.; and Senju Pharmaceutical Co, Ltd. Involved in management, analysis, interpretation, and preparation of the data (Y.I., M.I., T.R., T.H.) and interpretation and preparation of the manuscript (Y.I., M.I., A.H.). The study and data accumulation were carried out with approval from the Institutional Review Board of the Kyorin University School of Medicine and conformed to the tenets of the Declaration of Helsinki. Informed consent for the research was obtained from all patients. This clinical study has been registered (reference number NCT01306487) at <http://www.clinicaltrials.gov>.

REFERENCES

1. Benson WE, Cruickshanks KC, Fong DS, et al. Surgical management of macular holes: a report by the American Academy of Ophthalmology. *Ophthalmology* 2001;108(7):1328–1335.
2. Park DW, Sipperley JO, Sneed SR, Dugel PU, Jacobsen J. Macular hole surgery with internal-limiting membrane peeling and intravitreal air. *Ophthalmology* 1999;106(7):1392–1397.
3. Haritoglou C, Reiniger IW, Schaumberger M, et al. Five-year follow-up of macular hole surgery with peeling of the internal limiting membrane: update of a prospective study. *Retina* 2006;26(6):618–622.
4. Tranos PG, Ghazi-Nouri SM, Rubin GS, Adams ZC, Charteris DG. Visual function and subjective perception of visual ability after macular hole surgery. *Am J Ophthalmol* 2004;138(6):995–1002.
5. Sjaarda RN, Frank DA, Glaser BM, Thompson JT, Murphy RP. Resolution of an absolute scotoma and improvement of relative scotoma after successful macular hole surgery. *Am J Ophthalmol* 1993;116(2):129–139.
6. Christensen UC, Kroyer K, Sander B, et al. Value of internal limiting membrane peeling in surgery for idiopathic macular hole stage 2 and 3 - a randomized clinical trial. *Br J Ophthalmol* 2009;93(8):1005–1015.
7. Mester V, Kuhn F. Internal limiting membrane removal in the management of full-thickness macular holes. *Am J Ophthalmol* 2000;129(6):769–777.
8. Tognetto D, Grandin R, Sanguinetti G, et al. Macular Hole Surgery Study Group. Internal limiting membrane removal during macular hole surgery: results of a multicenter retrospective study. *Ophthalmology* 2006;113(8):1401–1410.

9. Leonard RE 2nd, Smiddy WE, Flynn HW Jr, Feuer W. Long-term visual outcomes in patients with successful macular hole surgery. *Ophthalmology* 1997;104(10):1648–1652.
10. Hangai M, Ojima Y, Gotoh N, et al. Three-dimensional imaging of macular holes with high-speed optical coherence tomography. *Ophthalmology* 2007;114(4):763–773.
11. Baba T, Yamamoto S, Arai M, et al. Correlation of visual recovery and presence of photoreceptor inner/outer segment junction in optical coherence images after successful macular hole repair. *Retina* 2008;28(3):453–458.
12. Chang LK, Koizumi H, Spaide RF. Disruption of the photoreceptor inner segment-outer segment junction in eyes with macular holes. *Retina* 2008;28(7):969–975.
13. Lee JE, Lee SU, Jea SY, Choi HY, Oum BS. Reorganization of photoreceptor layer on optical coherence tomography concurrent with visual improvement after macular hole surgery. *Korean J Ophthalmol* 2008;22(2):137–142.
14. Haritoglou C, Neubauer AS, Reiniger IW, et al. Long-term functional outcome of macular hole surgery correlated to optical coherence tomography measurements. *Clin Experiment Ophthalmol* 2007;35(3):208–213.
15. Christensen UC, Krøyer K, Sander B, Larsen M, la Cour M. Prognostic significance of delayed structural recovery after macular hole surgery. *Ophthalmology* 2009;116(12):2430–2436.
16. Inoue M, Watanabe Y, Arakawa A, et al. Spectral-domain optical coherence tomography images of inner/outer segment junctions and macular hole surgery outcomes. *Graefes Arch Clin Exp Ophthalmol* 2009;247(3):325–330.
17. Oh J, Smiddy WE, Flynn HW Jr, Gregori G, Lujan B. Photoreceptor inner/outer segment defect imaging by spectral domain OCT and visual prognosis after macular hole surgery. *Invest Ophthalmol Vis Sci* 2010;51(3):1651–1658.
18. Sano M, Shimoda Y, Hashimoto H, Kishi S. Restored photoreceptor outer segment and visual recovery after macular hole closure. *Am J Ophthalmol* 2009;147(2):313–318.
19. Oster SF, Mojana F, Brar M, et al. Disruption of the photoreceptor inner segment/outer segment layer on spectral domain-optical coherence tomography is a predictor of poor visual acuity in patients with epiretinal membranes. *Retina* 2010;30(5):713–718.
20. Otani T, Yamaguchi Y, Kishi S. Correlation between visual acuity and foveal microstructural changes in diabetic macular edema. *Retina* 2010;30(5):774–780.
21. Sakamoto A, Nishijima K, Kita M, et al. Association between foveal photoreceptor status and visual acuity after resolution of diabetic macular edema by pars plana vitrectomy. *Graefes Arch Clin Exp Ophthalmol* 2009;247(10):1325–1330.
22. Wakabayashi T, Oshima Y, Fujimoto H, et al. Foveal microstructure and visual acuity after retinal detachment repair. *Ophthalmology* 2009;116(3):519–528.
23. Shimoda Y, Sano M, Hashimoto H, Yokota Y, Kishi S. Restoration of photoreceptor outer segment after vitrectomy for retinal detachment. *Am J Ophthalmol* 2010;149(2):284–290.
24. Ota M, Tsujikawa A, Kita M, et al. Integrity of foveal photoreceptor layer in central retinal vein occlusion. *Retina* 2008;28(10):1502–1528.
25. Hayashi H, Yamashiro K, Tsujikawa A, et al. Association between foveal photoreceptor integrity and visual outcome in neovascular age-related macular degeneration. *Am J Ophthalmol* 2009;148(1):83–89.
26. Wakabayashi T, Fujiwara M, Sakaguchi H, Kusaka S, Oshima Y. Foveal microstructure and visual acuity in surgically closed macular holes: spectral-domain optical coherence tomographic analysis. *Ophthalmology* 2010;117(9):1815–1824.
27. Srinivasan VJ, Monson BK, Wojtkowski M, et al. Characterization of outer retinal morphology with high-speed, ultrahigh-resolution optical coherence tomography. *Invest Ophthalmol Vis Sci* 2008;49(4):1571–1579.
28. Park SJ, Woo SJ, Park KH, Hwang JM, Chung H. Morphologic photoreceptor abnormality in occult macular dystrophy on spectral-domain optical coherence tomography. *Invest Ophthalmol Vis Sci* 2010;51(7):3673–3679.
29. Imai M, Iijima H, Gotoh T, Tsukahara S. Optical coherence tomography of successfully repaired idiopathic macular holes. *Am J Ophthalmol* 1999;128(5):621–627.
30. Guérin CJ, Lewis GP, Fisher SK, Anderson DH. Recovery of photoreceptor outer segment length and analysis of membrane assembly rates in regenerating primate photoreceptor outer segments. *Invest Ophthalmol Vis Sci* 1993;34(1):175–183.
31. Michalewska Z, Michalewski J, Cisiecki S, Adelman R, Nawrocki J. Correlation between foveal structure and visual outcome following macular hole surgery: a spectral optical coherence tomography study. *Graefes Arch Clin Exp Ophthalmol* 2008;246(6):823–830.
32. Funata M, Wendel RT, de la Cruz Z, Green WR. Clinicopathologic study of bilateral macular holes treated with pars plana vitrectomy and gas tamponade. *Retina* 1992;12(4):289–298.
33. Madreperla SA, Geiger GL, Funata M, de la Cruz Z, Green WR. Clinicopathologic correlation of a macular hole treated by cortical vitreous peeling and gas tamponade. *Ophthalmology* 1994;101(4):682–686.
34. Ooto S, Hangai M, Sakamoto S, et al. High-resolution imaging of resolved central serous chorioretinopathy using adaptive optics scanning laser ophthalmoscopy. *Ophthalmology* 2010;117(9):1800–1809.
35. Gupta B, Laidlaw DA, Williamson TH, et al. Predicting visual success in macular hole surgery. *Br J Ophthalmol* 2009;93(11):1488–1491.



Biosketch

Yuji Ito, MD, PhD, is the Instructor of Ophthalmology, Kyorin Eye Center, Kyorin University School of Medicine, Tokyo, Japan. He has graduated at Oita University School of medicine in 2001 and has completed residencies in Ophthalmology at Oita University, Oita, Japan in 2003. He has been a vitreoretinal clinical fellow at Kyorin Eye Center, Tokyo, Japan since 2009. He has expertise in vitreoretinal diseases and surgery. His research interests are focused on researching vitreoretinal pathologies and molecular biology for vitreoretinal diseases.

Foveal Cone Outer Segment Tips Line and Disruption Artifacts in Spectral-Domain Optical Coherence Tomographic Images of Normal Eyes

TOSHO RII, YUJI ITOH, MAKOTO INOUE, AND AKITO HIRAKATA

• **PURPOSE:** To determine the incidence of a continuous cone outer segment tips (COST) line at the fovea in spectral-domain optical coherence tomographic (SD-OCT) images of normal eyes.

• **DESIGN:** Prospective, interventional case series.

• **METHODS:** Forty-six right eyes of 46 normal individuals with visual acuities (VA) $\geq 20/20$ were studied. SD-OCT images were obtained with a Cirrus HD-OCT instrument with both the standard 5-line raster and the high-definition (HD) 5-line raster scan modes. Images with signal strengths weaker than 5 (on a scale from 0 to 10) were excluded. The appearances of the COST line, photoreceptor inner segment/outer segment (IS/OS) junction, and external limiting membrane (ELM) line were determined in a masked way.

• **RESULTS:** The incidence of eyes with an intact foveal COST line was about 95%, and the incidence was not significantly associated with the age, sex, refractive error, signal strength, horizontal or vertical scans, and the use of either the standard or HD scans. Fragmented COST lines appeared to be attributable to blocking artifacts caused by a hyperreflectivity at the foveal surface because the COST fragmentation had corresponding fragmentation of the ELM and IS/OS junction lines. The correlation between a fragmented COST line and the hyperreflectivity on the retinal surface was significant for the vertical HD scans ($P = .011$) but not for the vertical standard, horizontal standard, or horizontal HD scans.

• **CONCLUSIONS:** Commercial SD-OCT instruments can detect the COST line. Fragmentations of the COST lines in normal eyes are most likely artifacts caused by a parabolic reflection of a surface hyperreflectivity of the foveal pit. (*Am J Ophthalmol* 2012;153:524–529. © 2012 by Elsevier Inc. All rights reserved.)

OPTICAL COHERENCE TOMOGRAPHY (OCT) IS A noninvasive imaging method that can provide cross-sectional images of the morphology of the retina with high resolution in real time.^{1–4} Quantitative and qualitative evaluations of the retinal microstructures are becoming a common diagnostic procedure in ophthalmology.

Accepted for publication Aug 6, 2011.

From Kyorin Eye Center, Kyorin University School of Medicine, Tokyo, Japan.

Inquiries to Makoto Inoue, Kyorin Eye Center, Kyorin University School of Medicine, 6-20-2 Shinkawa, Mitaka, Tokyo, 181-8611, Japan; e-mail: inoue@eye-center.org

Spectral-domain OCT (SD-OCT), which has better axial resolution than the conventional time-domain OCT (TD-OCT), has been used to evaluate the microstructures of the photoreceptors in eyes with different retinal pathologies.⁵ The restoration of the photoreceptor inner segment/outer segment (IS/OS) junction has been shown to be significantly correlated with the recovery of the visual acuity after surgery.^{6–14} It was suggested that the presence of a continuous IS/OS line was a sign of well-restored photoreceptor cells,¹² and a continuous external limiting membrane (ELM) was a sign of intact photoreceptor cell bodies in the outer nuclear layer and Müller cells.^{7,8}

Srinivasan and associates¹⁵ used high-speed, ultrahigh-resolution OCT to prove that the bright reflecting line located between the IS/OS junction and the retinal pigment epithelium in the ultrahigh-resolution OCT images was the boundary of the cone outer segment tips (COST). This highly reflective line has also been called the Verhoeff membrane;^{16,17} however, histopathologic correlation has been under investigation.

The relationship between the visual acuity and the integrity of the foveal COST line detected by commercial SD-OCTs has been reported in cases of occult macular dystrophy.^{16,18} In addition, we recently reported a significant correlation between the visual acuity and the integrity of foveal COST line after successful macular hole surgery.¹⁹ The recovery of the COST line was observed only in eyes with an intact IS/OS junction and ELM line. Eyes with postoperative visual acuity $\geq 20/25$ at postoperative 12 months were more frequently associated with the eyes with a recovered COST line.¹⁹

The microstructures of the outer retina detected by commercial OCT instruments in normal subjects have not been well evaluated. We believe that it is essential to determine whether these commercial SD-OCT instruments can detect the foveal microstructures of normal subjects before applying these techniques to study eyes with vitreoretinal pathologies.

Thus, the aim of this study was to determine the incidence of a continuous COST line at the fovea of normal eyes using a commercial SD-OCT instrument. In addition, we determined which parameters of the SD-OCT would be best to use to obtain good-quality images of the COST line. The possible reasons why abnormal COST

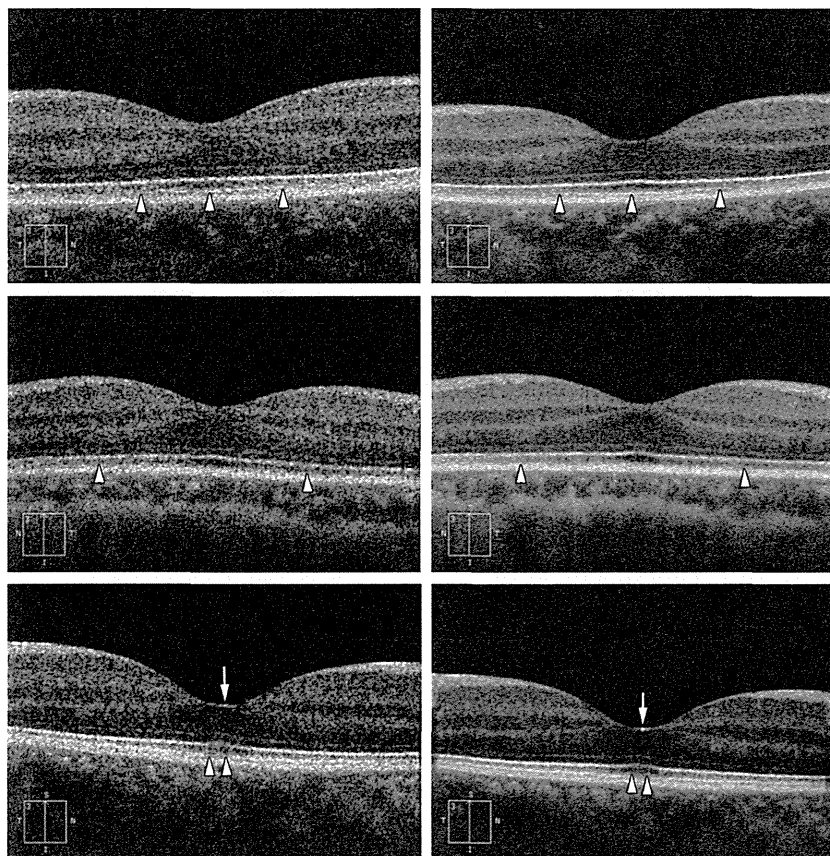


FIGURE 1. Magnified spectral-domain optical coherence tomographic image of a vertical scan of a normal fovea. (Top) Standard scan of a 30-year-old woman with a refractive error of -5.0 diopters (D) and an axial length of 25.4 mm showing a continuous cone outer segment tips (COST) line (arrowheads) in the standard scan (left) and also in the high-definition scan (right). (Middle) COST line is absent (arrowheads) at the fovea of a 34-year-old man with a refractive error of -3.75 D and an axial length of 26.0 mm in the standard scan (left) and high-definition scan (right). (Bottom) COST line is fragmented (arrowheads) at the fovea of a 25-year-old woman with a refractive error of -1.5 D and an axial length of 24.5 mm with a hyperreflectivity at the foveal surface (arrow) in the standard scan (left) and high-definition scan (right).

lines, IS/OS junctions, and ELM signals were present in the OCT images were also investigated.

PATIENTS AND METHODS

FORTY-SIX EYES OF 46 HEALTHY VOLUNTEERS (19 MEN AND 27 women) without any eye diseases were studied. The right eye of each subject was chosen arbitrarily to study. Each subject had a routine eye examination including measurements of the best-corrected visual acuity (BCVA) and intraocular pressure. All of the subjects had a BCVA of $\geq 20/20$.

SD-OCT images were obtained by 6-mm scans with the Cirrus HD-OCT instrument (OCT 4000, Carl Zeiss Meditec, Dublin, California, USA) with both the standard 5-line raster scan (standard scan) and the high-definition (HD) 5-line raster scan (HD scan). We recorded both 6-mm horizontal and vertical scans to evaluate the integrity of the COST line, the ELM, and the IS/OS junction in the foveal region. The images were magnified with the built-in zoom function to evaluate the foveal microstruc-

tures. Three experienced investigators (T.R., Y.I., M.I.) who were masked to the subjects' ophthalmologic data, including age and refractive errors, evaluated the SD-OCT images. Images with signal strength weaker than 5 (on a scale from 0 to 10) were excluded. The demographic data of the subjects, refractive errors (spherical equivalent) of the eyes, and signal strengths of the OCT images were recorded.

For statistical analysis, Student *t* tests, Welch *t* tests, Kruskal-Wallis tests, and 1-way analysis of variance (ANOVA) were used. A *P* value of .05 was set as significant.

RESULTS

THE MEAN AGE OF THE SUBJECTS WAS 33.0 YEARS WITH A range from 23 to 50 years. The mean decimal BCVA was 1.1 with a range from 1.0 to 1.5. The mean refractive error was -1.49 diopters (D) with a range from -8.0 to $+3.25$ D. The intraocular pressure ranged from 12 to 18 mm Hg. The mean signal strengths were 8.2 (horizontal standard

TABLE 1. Incidence and Characteristics of Eyes With Continuous, Fragmented, or Absent Cone Outer Segment Tips Line

	Standard Scan (n = 45)				HD Scan (n = 46)			
	Continuous COST Line	Fragmented COST Line	Absent COST Line	P Value	Continuous COST Line	Fragmented COST Line	Absent COST Line	P Value
Horizontal scan								
No. (%) eyes	43 (96%)	0	2 (4%)	n/a	43 (93%)	1 (2%)	2 (4%)	n/a
Age (mean, y)	33.3	n/a	32.5	.882 ^a	33.1	41.0	32.5	.503 ^b
Sex (M:F)	18:25	n/a	1:1	>.999 ^c	18:25	0:1	1:1	>.999 ^c
Signal strength (mean)	8.3	n/a	7.0	.130 ^a	8.4	9.0	7.0	.225 ^b
Refractive error (mean, diopters)	-1.44	n/a	-3.25	.335 ^a	-1.45	0.00	-3.25	.262 ^b
Vertical scan								
No. (%) eyes	39 (91%)	2 (5%)	2 (5%)	n/a	38 (88%)	3 (7%)	2 (5%)	n/a
Age (mean, y)	34.0	25.0	32.5	.144 ^b	33.1	37.3	32.5	.718 ^b
Sex (M:F)	16:23	0:2	1:1	.761 ^c	17:21	0:3	1:1	.376 ^c
Signal strength (mean)	8.3	8.5	7.5	.451 ^b	8.3	8.7	8.0	.724 ^b
Refractive error (mean, diopters)	-1.51	-0.75	-3.25	.369 ^b	-1.60	+0.17	-3.25	.217 ^b

COST = cone outer segment tips; HD scan = high-definition 5-line raster scan; Standard scan = standard 5-line raster scan.
^aStudent *t* test.
^bKruskal-Wallis 1-way analysis of variance.
^cFreeman-Halton extension of the Fisher exact probability test.

scan), 8.3 (vertical standard scan), 8.3 (horizontal HD scan), and 8.3 (vertical HD scan); the range of signal strength was from 6 to 10.

In the SD-OCT images, the COST line was recognized as a continuous line located between the IS/OS line and the retinal pigment epithelium layer (Figure 1). The COST line at the fovea was classified as continuous, fragmented, or absent. In 2 eyes where the COST line was absent and 20 eyes where a continuous COST line was detected, the OCT examination was repeated at different times of the day and on different days in a masked way. In all cases, the findings were the same in all eyes, and the repeatability of detecting a COST line was confirmed. In the 2 eyes with an absent COST line, the foveal COST line was absent for up to 6 months.

The incidence of detecting a COST line (continuous COST and fragmented COST) was 43 of 45 eyes (96%) in the horizontal standard scans, 41 of 43 eyes (95%) in the vertical standard scans, 44 of 46 eyes (96%) in the horizontal HD scans, and 41 of 43 eyes (95%) in the vertical HD scans (Table 1). The range of detecting a continuous COST line was between 88% and 96% and a continuous COST line, but with fragmentation at the fovea (fragmented COST line), was between 0% and 7%. The differences in the incidences of a continuous COST line between the horizontal and vertical scans were not significant in either the standard or the HD scans ($P = .429$, $P = .475$, respectively, Fisher exact probability test). The differences in the incidences of detecting a continuous COST line between the standard scans and the

HD scans were also not significant in either the horizontal or the vertical scans ($P > .999$, $P > .999$, respectively). The 2 eyes with an absent COST line were the same eyes in horizontal or vertical scan and standard or HD scan. One of these 2 eyes was that of a 31-year-old woman and the other that of a 34-year-old man. The refractive errors were -2.75 D and -3.75 D and the axial lengths measured by OA1000 (TOMEY Corp, Nagoya, Japan) were 26.1 mm and 26.0 mm. The age, sex, signal strengths, and refractive errors were not significantly different among the eyes with a continuous, fragmented, or absent COST line (Table 1).

In all of the eyes with a fragmented COST line, a hyperreflective signal was seen at the surface of the foveal pit with weaker signals behind. These signals in both the standard and HD scans resembled the "acoustic shadow" artifacts that are observed in ultrasound echography (Figure 2). The signal intensities of the ELM, IS/OS junction, and COST lines at the fovea behind the hyperreflectivity were weaker and the lines were clearly fragmented. The diameter of the weaker signals behind the hyperreflectivity was wider in the lower (scleral) direction.

A fragmented COST line was always associated with the hyperreflectivity at the foveal pit surface (horizontal HD scans, $P = .227$; vertical standard scans, $P = .055$; vertical HD scans, $P = .011$, Fisher exact probability test, Table 2) and fragmented signals of the ELM (horizontal HD scans, $P = .098$; vertical standard scans, $P = .001$; vertical HD scans, $P < .001$) and IS/OS junction (horizontal HD scans, $P = .068$; vertical standard scans, $P = .001$; vertical HD

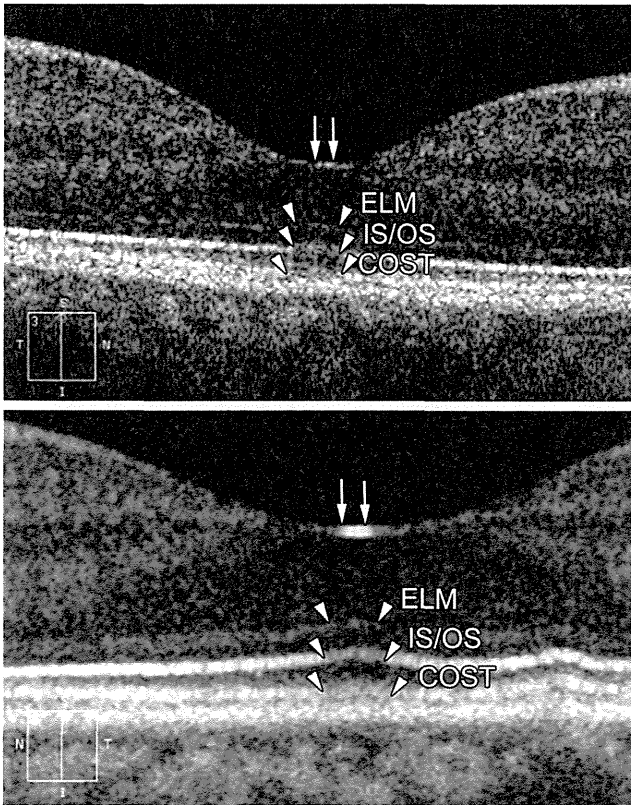


FIGURE 2. Magnified spectral-domain optical coherence tomographic images in eyes with hyperreflectivity at the foveal pit surface. Hyperreflective areas at the foveal pit surface (arrows) are seen in (Top) standard scan and (Bottom) high-definition scan in a 41-year-old woman who was emmetropic and had an axial length of 22.5 mm. Behind the hyperreflectivity, the signal intensities of the external limiting membrane (ELM), inner segment/outer segment junction (IS/OS), and cone outer segment tips (COST) are reduced (arrowheads). The diameter of the reduced signals behind the hyperreflectivity becomes wider in the lower direction.

scans, $P < .001$). A fragmented IS/OS junction line was also found in eyes with hyperreflectivity at the foveal surface (horizontal standard scans, $P = .017$; horizontal HD scans, $P = .009$; vertical standard scans, $P = .055$; vertical HD scans, $P = .011$) and fragmented ELM line (horizontal standard scans, $P = .001$; horizontal HD scans, $P < .001$; vertical standard scans, $P = .001$; vertical HD scans, $P < .001$). A fragmented ELM line was also associated with the hyperreflectivity (horizontal standard scans, $P = .017$; horizontal HD scans, $P = .002$; vertical standard scans, $P = .055$; vertical HD scans, $P < .001$).

The fragmented signals of the COST, IS/OS junction, and ELM lines were dependent on the depth of the acoustic shadows beneath the hyperreflective areas. Thus, a fragmented COST line was considered to be an artifact caused by the hyperreflectivity at the foveal pit surface. Consequently, a fragmented COST line can be considered to be an intact foveal COST line with artifacts. The incidence of an intact foveal COST line with

or without artifacts was 95% to 96%. There were no significant differences in detecting an intact foveal COST line in the standard or the HD scan modes (horizontal scans, $P > .999$; vertical scans, $P > .999$), and in the vertical or the horizontal scans (standard scans, $P > .999$; HD scans, $P > .999$).

DISCUSSION

THE CORRELATIONS BETWEEN THE VISUAL ACUITY AND the integrity of the foveal COST line detected by commercial SD-OCT instruments has been reported to be significant in cases of occult macular dystrophy,^{16,18} adult-onset foveomacular vitelliform dystrophy,¹⁷ macular hole,¹⁹ and central serous chorioretinopathy.²⁰ Morphologic changes including an absence of the foveal COST line in the SD-OCT images have been reported to be correlated with the condition of the retina in eyes with retinal diseases.^{16–20} However, we found an absent COST line at the fovea in 4% to 5% of normal eyes.

The resolution of the SD-OCT we used was $5\ \mu\text{m}$,¹⁵ and we found a COST line in approximately 95% of the normal subjects. If we assume that a continuous COST line is the normal condition in normal eyes, this suggests that commercially available SD-OCT instruments with $5\text{-}\mu\text{m}$ resolution can determine the condition of the COST line in 95% of normal eyes.

Our observations indicate that the fragmentation was most likely an artifact caused by a hyperreflectivity at the foveal pit surface casting acoustic shadows. The hyperreflectivity was always found at the foveal pit surface, and we assumed that the hyperreflectivity was caused by a parabolic reflection from the surface of the foveal pit. The hyperreflectivity in the fovea is different from the hyperreflective area described for a closed macular hole after successful macular hole surgery because the hyperreflectivity was observed at the surface of the fovea.⁷

Eyes with a fragmentation of the COST line also had fragmentation or disruption of the IS/OS junction and ELM lines. We suggest that these fragmentations are acoustic shadows, as has been described for retinal vessels in SD-OCT images.^{3,21} In addition, vitreous opacities such as asteroid bodies in eyes with asteroid hyalosis or intraretinal exudates such as hard exudates can also result in similar-appearing acoustic shadows.^{3,21,22} Such opacities cause signal attenuation in the underlying tissues including the retina, retinal pigment epithelium, and choroid. The hyperreflectivity at the foveal pit surface may cause a similar effect in eyes with a fragmented COST line. Depending on the depth of the acoustic shadows, the ELM, IS/OS, and COST lines can appear fragmented. However, the area of reduced COST signals was very small and can only be seen with magnification in the macular area. This may be the reason why these artifacts have not been reported. However, the possibility of this kind of artifact

TABLE 2. Incidence of Fragmented Signals and Hyperreflectivity at the Foveal Surface

	Standard Scan (n = 43)			HD Scan (n = 44)		
	HR+	HR-	P Value ^a	HR+	HR-	P Value ^a
Horizontal scan						
ELM line						
Continuous	4 (9%)	37 (86%)	.017	6 (14%)	34 (77%)	.002
Fragmented	2 (5%)	0		4 (9%)	0	
IS/OS junction						
Continuous	4 (9%)	37 (86%)	.017	7 (16%)	34 (77%)	.009
Fragmented	2 (5%)	0		3 (7%)	0	
COST line						
Continuous	6 (14%)	37 (86%)	>.999	9 (20%)	34 (77%)	.227
Fragmented	0	0		1 (2%)	0	
<!---->Vertical scan						
ELM line						
Continuous	8 (20%)	31 (76%)	.055	5 (12%)	31 (76%)	<.001
Fragmented	2 (5%)	0		5 (12%)	0	
IS/OS junction						
Continuous	8 (20%)	31 (76%)	.055	7 (17%)	31 (76%)	.011
Fragmented	2 (5%)	0		3 (7%)	0	
COST line						
Continuous	8 (20%)	31 (76%)	.055	7 (17%)	31 (76%)	.011
Fragmented	2 (5%)	0		3 (7%)	0	

COST = cone outer segment tips; ELM = external limiting membrane; HD scan = high-definition 5-line raster scan; HR = hyperreflectivity; IS/OS = inner segment/outer segment junction; Standard scan = standard 5-line raster scan.

^aFisher exact probability test.

should be remembered when evaluating the continuity of the foveal microstructures.

Artifacts represent a major concern of every imaging method. Because of the Fourier transformation of the SD-OCT signals, the real image is always inverted.^{23,24} A mirror artifact is often detected in patients with moderate to high myopia and is responsible for the “pseudo” small, round retinal lesions located in the outer plexiform layer. In eyes with asteroid hyalosis, the mirror artifacts from a shadowing effect by the asteroid bodies result in an inverted image not only in the deeper layers but even in the superficial layers.²⁴ Although SD-OCT is a significant advance in the imaging of the retina, artifacts are still present and can still influence clinical decisions.

Our study showed that the COST line was not detected in approximately 5% of the normal eyes and these eyes did not have any artifacts including hyperreflectivity at the foveal surface. The photoreceptors are in a dynamic state of adding and shedding outer segments.²⁵ The foveal microstructures of the outer segments appear to be related to the functional status of the photoreceptors and to the visual acuity. Light-induced retinal damage is well recognized.²⁶ Even ambient light can damage murine cones in a

rhodopsin mutant retina, and subsequent light restriction led to recovery of the damaged cones and rods.²⁷ Prolonged visual activities such as gazing at a computer display may cause photoreceptor damage, with moderate visual impairment and disrupted IS/OS line detected by SD-OCT.²⁸ A decrease in the length of the outer segments of the cones by prolonged visual activities may result in indistinct COST line even in normal subjects. After the patients stopped prolonged visual activities, vision recovered to normal but it took 3 to 16 weeks. In our study, repeated OCT examinations at different times of the day up to 6 months showed good repeatability of the SD-OCT images. We also took SD-OCT images immediately after the subjects were awake in which the condition was compatible with the effect of light restriction. For eyes in which the COST line cannot be detected, more studies are needed to find out the cause of the absent COST line.

In conclusion, commercially available SD-OCT instruments can be used to evaluate the microstructures of the outer retinal layers, including the COST line. However, it should be noted that the COST line may be fragmented or absent even in normal eyes. More studies are needed to determine the characteristics of the eyes with absent COST lines.

THE AUTHORS INDICATE NO GOVERNMENT OR NONGOVERNMENT FINANCIAL SUPPORT FOR THIS ARTICLE. DR INOUE HAS received speaker support from Alcon Japan, Ltd; Santen Pharmaceutical Inc; HOYA Corp, and Kowa Pharmaceutical Co Ltd. Dr Hirakata has received speaker support from Alcon Japan, Ltd; Santen Pharmaceutical Inc; Novartis Pharma K.K.; and Senju Pharmaceutical Co, Ltd. Involved in management, analysis, interpretation, and preparation of the data (T.R., Y.L., M.I.); and in interpretation and preparation of the manuscript (T.R., Y.L., M.I., A.H.). The study and data accumulation were carried out with approval from the Institutional Review Board of the Kyorin University School of Medicine and conformed to the tenets of the Declaration of Helsinki. Informed consent for the research was obtained from all patients. This clinical study has been registered with a reference number of NCT01316003 at <http://www.clinicaltrials.gov>.

REFERENCES

1. Huang D, Swanson EA, Lin CP, et al. Optical coherence tomography. *Science* 1991;(5035):1178–1181.
2. Puliafito CA, Hee MR, Lin CP, et al. Imaging of macular diseases with optical coherence tomography. *Ophthalmology* 1995;102(2):217–229.
3. Schuman, JS. Puliafito CA. Fujimoto JG. *Optical Coherence Tomography of Ocular Diseases*. 2nd ed. Slack Inc; Thorofare, NJ: 2004.
4. Ishikawa H, Stein DM, Wollstein G, et al. Macular segmentation with optical coherence tomography. *Invest Ophthalmol Vis Sci* 2005;46(6):2012–2017.
5. Hangai M, Ojima Y, Gotoh N, et al. Three-dimensional imaging of macular holes with high-speed optical coherence tomography. *Ophthalmology* 2007;114(4):763–773.
6. Otani T, Yamaguchi Y, Kishi S. Correlation between visual acuity and foveal microstructural changes in diabetic macular edema. *Retina* 2010;30:774–780.
7. Wakabayashi T, Fujiwara M, Sakaguchi H, Kusaka S, Oshima Y. Foveal microstructure and visual acuity in surgically closed macular holes: spectral-domain optical coherence tomographic analysis. *Ophthalmology* 2010;117(9):1815–1824.
8. Wakabayashi T, Oshima Y, Fujimoto H, et al. Foveal microstructure and visual acuity after retinal detachment repair. *Ophthalmology* 2009;116(3):519–528.
9. Baba T, Yamamoto S, Arai M, et al. Correlation of visual recovery and presence of photoreceptor inner/outer segment junction in optical coherence images after successful macular hole repair. *Retina* 2008;28(3):453–458.
10. Chang LK, Koizumi H, Spaide RF. Disruption of the photoreceptor inner segment-outer segment junction in eyes with macular holes. *Retina* 2008;28(7):969–975.
11. Lee JE, Lee SU, Jea SY, Choi HY, Oum BS. Reorganization of photoreceptor layer on optical coherence tomography concurrent with visual improvement after macular hole surgery. *Korean J Ophthalmol* 2008;22(2):137–142.
12. Shimoda Y, Sano M, Hashimoto H, Yokota Y, Kishi S. Restoration of photoreceptor outer segment after vitrectomy for retinal detachment. *Am J Ophthalmol* 2010;149(2):284–290.
13. Michalewska Z, Michalewski J, Cisiecki S, Adelman R, Nawrocki J. Correlation between foveal structure and visual outcome following macular hole surgery: a spectral optical coherence tomography study. *Graefes Arch Clin Exp Ophthalmol* 2008;246(6):823–830.
14. Oster SF, Mojana F, Brar M, et al. Disruption of the photoreceptor inner segment/outer segment layer on spectral domain-optical coherence tomography is a predictor of poor visual acuity in patients with epiretinal membranes. *Retina* 2010;30(5):713–718.
15. Srinivasan VJ, Monson BK, Wojtkowski M, et al. Characterization of outer retinal morphology with high-speed, ultrahigh-resolution optical coherence tomography. *Invest Ophthalmol Vis Sci* 2008;49(4):1571–1579.
16. Park SJ, Woo SJ, Park KH, Hwang JM, Chung H. Morphologic photoreceptor abnormality in occult macular dystrophy on spectral-domain optical coherence tomography. *Invest Ophthalmol Vis Sci* 2010;51(7):3673–3679.
17. Puche N, Querques G, Benhamou N, et al. High-resolution spectral domain optical coherence tomography features in adult onset foveomacular vitelliform dystrophy. *Br J Ophthalmol* 2010;94(9):1190–1196.
18. Sisk RA, Berrocal AM, Lam BL. Loss of foveal cone photoreceptor outer segments in occult macular dystrophy. *Ophthalmic Surg Lasers Imaging* 2010. Forthcoming.
19. Itoh Y, Inoue M, Rii T, Hiraoka T, Hirakata A. Significant correlation between visual acuity and recovery of foveal cone microstructures after macular hole surgery. *Am J Ophthalmol* 2011. Forthcoming.
20. Ooto S, Hangai M, Sakamoto S, et al. High-resolution imaging of resolved central serous chorioretinopathy using adaptive optics scanning laser ophthalmoscopy. *Ophthalmology* 2010;117(9):1800–1809.
21. Hee MR, Fujimoto JG, Ko T, et al. Interpretation of the optical coherence tomography image. In: Shuman JS, Puliafito CA, Fujimoto JG, eds. *Optical coherence tomography of ocular diseases*. 2nd ed. Thorofare, NJ: SLACK Incorporated; 2004:21–56.
22. Han IC, Jaffe GJ. Evaluation of artifacts associated with macular spectral-domain optical coherence tomography. *Ophthalmology* 2010;117(6):1177–1189.
23. Ho J, Castro DP, Castro LC, et al. Clinical assessment of mirror artifacts in spectral-domain optical coherence tomography. *Invest Ophthalmol Vis Sci* 2010;51(7):3714–3720.
24. Querques G, Forte R, Querques L, Souied EH. Artifacts associated with spectral-domain OCT. *Ophthalmology* 2011; 118(1):222.
25. Guérin CJ, Lewis GP, Fisher SK, Anderson DH. Recovery of photoreceptor outer segment length and analysis of membrane assembly rates in regenerating primate photoreceptor outer segments. *Invest Ophthalmol Vis Sci* 1993;34(1):175–183.
26. Wu J, Seregard S, Algvere PV. Photochemical damage of the retina. *Surv Ophthalmol* 2006;51(5):461–481.
27. Chrysostomou V, Stone J, Stowe S, Barnett NL, Valter K. The status of cones in the rhodopsin mutant P23H-3 retina: light-regulated damage and repair in parallel with rods. *Invest Ophthalmol Vis Sci* 2008;49(3):1116–1125.
28. Kishi S, Li D, Takahashi M, Hashimoto H. Photoreceptor damage after prolonged gazing at a computer game display. *Jpn J Ophthalmol* 2010;54(5):514–516.



Biosketch

Tosho Rii a.k.a. Tong-Sheng Lee, MD, is currently an Instructor of Ophthalmology, Kyorin University Medical School, Tokyo, Japan. He received his MD from China Medical University, Taiwan, in 1997 and completed his ophthalmology residency at Shin Kong Wu Ho-Su Memorial Hospital, Taipei, Taiwan. He gained laboratory research experiences in Taipei Medical University and Osaka University, and then joined the vitreo-retinal services of the Kyorin Eye Center in 2010. Dr Rii's research interest is in the pathophysiology and imaging of vitreoretinal diseases.

Correlation between Length of Foveal Cone Outer Segment Tips Line Defect and Visual Acuity after Macular Hole Closure

Yuji Itoh, MD, Makoto Inoue, MD, Toshi Rii, MD, Tomoyuki Hiraoka, MD, Akito Hirakata, MD

Purpose: To determine whether the postoperative length of the photoreceptor cone outer segment tips (COST) line defect is significantly correlated with best-corrected visual acuity (BCVA) after macular hole closure.

Design: Retrospective, consecutive, observational case series.

Participants: Fifty-one eyes of 51 patients with a surgically closed macular hole were studied.

Methods: Spectral-domain optical coherence tomography (SD-OCT) was used to obtain images of the foveal area, and the lengths of the COST line defect were measured in the images obtained 1, 3, 6, 9, and 12 months after macular hole surgery. The correlation between the length of COST line defect and the BCVA was determined.

Main Outcome Measures: The lengths of the COST line defect, the inner segment/outer segment (IS/OS) junction defect, the external limiting membrane (ELM) line defect in the SD-OCT images, and the BCVA.

Results: The COST line defect was gradually restored centripetally 1 to 12 months postoperatively. The length of the COST line defect was significantly correlated with the BCVA at 1, 3, 6, 9, and 12 months postoperatively ($P < 0.001$). Forward stepwise regression analyses showed that the postoperative BCVA was significantly correlated with the length of the COST line defect ($P < 0.001$) but not with that of the IS/OS junction and ELM line defects after 6 months. The preoperative length of the COST line defect was significantly correlated with postoperative BCVA at 12 months ($P = 0.020$), but the length of the IS/OS junction and ELM line defects was not. The preoperative length of the COST line defect was significantly longer than the fluid cuff diameter of the macular hole ($P = 0.020$), indicating that the influence of the elevated neurosensory retina at the fluid cuff on the SD-OCT signals of the COST line was probably minimal. The postoperative BCVA at 12 months can be calculated by the following regression equation: $BCVA = 0.00020 \times (\text{length of preoperative COST line defect } [\mu\text{m}]) - 0.23$ (F value = 15.4; $P < 0.001$).

Conclusions: The recovery of the foveal COST line defect is related to visual recovery after macular hole closure. The length of the preoperative COST line defect may predict the BCVA after macular hole surgery.

Financial Disclosure(s): Proprietary or commercial disclosure may be found after the references. *Ophthalmology* 2012;119:1438–1446 © 2012 by the American Academy of Ophthalmology.



Spectral-domain optical coherence tomography (SD-OCT) has better resolution than earlier optical coherence tomography (OCT) instruments, and this has allowed clinicians to evaluate the microstructure of the photoreceptors more precisely.^{1–3} The effect of an idiopathic macular hole on the foveal microstructures has been evaluated by SD-OCT before and after successful closure of the macular hole.^{4–13} The presence of a continuous photoreceptor inner segment/outer segment (IS/OS) line is a sign of well-restored photoreceptor cells,^{12,13} and the restoration of the photoreceptor IS/OS junction is significantly correlated with the recovery of visual acuity after surgery.^{5,7} The recovery of the IS/OS junction progresses from the periphery toward the center of the closed macular hole, and the total area and length of the IS/OS junction defect after surgery are significantly correlated with postoperative visual acuity.^{10,11,14,15} The recovery of the external limiting membrane (ELM) is also correlated with the recovery of visual acuity after macular hole closure.¹⁶

High-speed, ultra-high-resolution OCT has been used to acquire, measure, and map the outer retinal morphology, including the topographic distribution of cone and rod photoreceptors in the macula area.¹⁷ On the ultra-high-resolution OCT images, a highly reflective line was detected between the IS/OS junction and the bright retinal pigment epithelium line. This line has been identified as the border of the cone outer segment tips (COST) and has thus been named the “COST line.”

We previously reported that a significant correlation exists between postoperative visual acuity and integrity of the foveal COST line after successful macular hole surgery.¹⁸ The recovered COST line was observed only in eyes with an intact IS/OS junction and ELM line. The eyes with visual acuity $\geq 20/25$ at 12 months postoperatively were more frequently (91%) associated with eyes with a recovered COST line.¹⁸ However, we did not analyze whether the length of the foveal COST line defect was significantly correlated

with postoperative visual acuity. In addition, the associations between preoperative factors of photoreceptor microstructure and postoperative vision were not determined.

The purposes of the current study were (1) to determine whether the length of the postoperative COST line defect is significantly correlated with best-corrected visual acuity (BCVA) before and after successful macular hole surgery, and (2) to determine the preoperative factors that are significantly associated with postoperative BCVA.

Patients and Methods

The medical records of 72 eyes of 72 consecutive patients with a surgically closed idiopathic macular hole at the final visit were reviewed. All patients were diagnosed with a stage 2, 3, or 4 idiopathic macular hole according to the Gass classification and had undergone surgery between March 2008 and February 2010 at Kyorin Eye Center. Preoperative data included age, gender, right or left eye, axial length, stage of macular hole, symptom duration, Snellen BCVA, macular hole diameter, length of the COST line defect, and length of the IS/OS and ELM defects were recorded.

All patients had comprehensive ophthalmologic examinations before and at 1, 3, 6, 9, and 12 months after the surgery. The examinations included measurements of the BCVA, fundus examinations by binocular indirect ophthalmoscopy and non-contact lens slit-lamp biomicroscopy, fundus photography, and fundus autofluorescence imaging by confocal scanning ophthalmoscopy (Heidelberg Retina Angiograph 2, Heidelberg Engineering, Heidelberg, Germany). The SD-OCT examination was performed on all patients on the same day as the clinical examinations. The length of the COST line defect was measured on the SD-OCT images.

All surgeries were performed after the patients received a detailed explanation of the surgical and SD-OCT procedures. Informed consent was obtained from all patients, and the procedures adhered to the tenets of the Declaration of Helsinki. The study protocol was approved by the institutional review committee of the Kyorin University School of Medicine, and all patients consented to the review of their medical records. This clinical study has been registered at the US National Institutes of Health (www.clinicaltrials.gov) as "Foveal Cone Outer Segment Resumption to Predict Visual Recovery after Macular Hole Surgery," with a reference number of NCT01381965. The main outcome measures were the 12-month postoperative BCVA and the condition of the foveal microstructures in the SD-OCT images.

The surgery was performed by 1 of the 3 retina specialists (T.H., M.I., A.H.). A standard 3-port pars plana vitrectomy was used to close the macular hole with 2% lidocaine retrobulbar anesthesia. An intravitreal injection of triamcinolone acetonide (Kenacort-A, Bristol Pharmaceuticals KK, Tokyo, Japan) or indocyanine green (Santen Pharmacy, Osaka, Japan) was performed to make the vitreous gel and internal limiting membrane (ILM) more visible. Core vitrectomy was performed with the creation of a posterior vitreous detachment if it was not present, and the ILM was removed in all cases. The lens was extracted from all patients aged >55 years. In addition, all cataractous lenses were removed by phacoemulsification with an implantation of an intraocular lens. Room air or nonexpansive 20% sulfur hexafluoride was used to tamponade the retina, and patients were instructed to maintain a face-down position for 3 to 4 days postoperatively. Anatomic success was defined as the presence of a closed macular hole at 1 month postoperatively as confirmed by slit-lamp biomicroscopy and SD-OCT and the absence of autofluorescence at the site of the macular hole.

Spectral-domain OCT (OCT4000, Cirrus HD-OCT, Carl Zeiss Meditec Inc, Dublin, CA) was used to obtain tomographic images

of the macular area. The entire macular area was scanned, and high-quality 6-mm scan images were obtained with the 5-line raster mode or high-definition 5-line raster mode. The diameter of the macular hole was taken to be the distance of the neurosensory retinal defect, and the mean values of the distance in the vertical and horizontal images at the fovea were evaluated. The diameter of fluid cuff around the macular hole was defined as the maximal distance between the edges of the neurosensory retina detached from the retinal pigment epithelium. The mean length of the COST line defect, preoperative IS/OS line defect, ELM defect, and fluid cuff was calculated by averaging the vertical and horizontal lengths of the defects with the software embedded in the SD-OCT system. Two experienced investigators (Y.I., T.R.), who were masked to the patients' information, including the postoperative period and BCVA, independently measured each of the parameters on each SD-OCT image. Scans with a signal strength >8/10 were examined, and a high-quality representative image was selected for the measurements. The axial length of the eye was measured preoperatively with the OA1000 (TOMEY Corp, Nagoya, Japan).

The decimal BCVA was converted to logarithm of the minimal angle of resolution (logMAR) units for the statistical analysis. To compare preoperative and postoperative values, Student *t* tests were used with continuous data. Pearson's correlation coefficient tests were performed to evaluate the agreement between the 2 investigators who measured the length of the COST line defect on each SD-OCT image. Multivariable analysis was also used to investigate the relationships between preoperative and postoperative length of the COST line, IS/OS junction, and ELM line defects, and the BCVA at 3, 6, 9, and 12 months. Simple linear regression analysis was used to determine the correlation between postoperative BCVA and preoperative or postoperative length of the COST line defect. The lengths of the COST line defect, IS/OS junction defect, ELM defect, and fluid cuff at each period were evaluated by 1-way analysis of variance and post hoc test. Forward stepwise regression analysis was performed to determine whether the age, gender, symptom duration, axial length, stage of macular hole, and preoperative BCVA were significantly associated with the BCVA at 12 months after the surgery.

Table 1. Patient Baseline Characteristics

No. of eyes (patients)	51 (51)
Age (yrs) (mean ± SD; range)	65.5 ± 7.3 (47–83)
Gender, no. (%)	
Men	20 (39%)
Women	31 (61%)
Eye, no. (%)	
Right	28 (55%)
Left	23 (45%)
Axial length (mm; mean ± SD)	23.7 ± 1.1
Preoperative BCVA (logMAR; mean ± SD)	0.56 ± 0.24
Symptom duration (mos; mean ± SD; range)	4.6 ± 4.3 (1–18)
Preoperative stage, no. (%)	
stage 2	14 (28%)
stage 3	33 (65%)
stage 4	4 (7%)
Preoperative diameter of the hole (μm) (mean ± SD; range)	336 ± 152 (136–946)
Types of gas tamponade for PPV, no. (%)	
Air	19 (37%)
SF ₆	32 (63%)
Combination of cataract surgery, no. (%)	46 (90%)

BCVA = best-corrected visual acuity; logMAR = logarithm of the minimum angle of resolution; PPV = pars plana vitrectomy; SD = standard deviation; SF₆ = sulfur hexafluoride.

Results

Of the original 72 eyes, 12 were excluded because of the presence of retinal diseases, including a treated rhegmatogenous retinal detachment, diabetic retinopathy, and high myopia with an axial length >27.0 mm or refractive error >-8.0 diopters (D). Nine other eyes were excluded because they were not followed for at least 6 months postoperatively at the Kyorin Eye Center, Kyorin University School of Medicine. In total, 51 eyes of 51 patients (20 men, 31 women) met the study criteria for the data analyses.

The preoperative baseline characteristics of the 51 eyes are summarized in Table 1. The mean age was 65.5 ± 7.3 years (range, 47–83 years). The average refractive error of the 48 phakic eyes was -1.3 D (range, -7.0 to $+3.5$ D). The mean preoperative decimal BCVA was 0.27 (Snellen equivalent, 20/80; 0.56 logMAR units). The mean postoperative follow-up time was 11.8 months (range, 6–19 months). The interval between the onset of visual symptoms and the macular hole surgery ranged from 1 to 18 months, with a mean of 4.6 months. The mean axial length of 48 of the phakic eyes was 23.7 mm (range, 21.2–26.8 mm). The

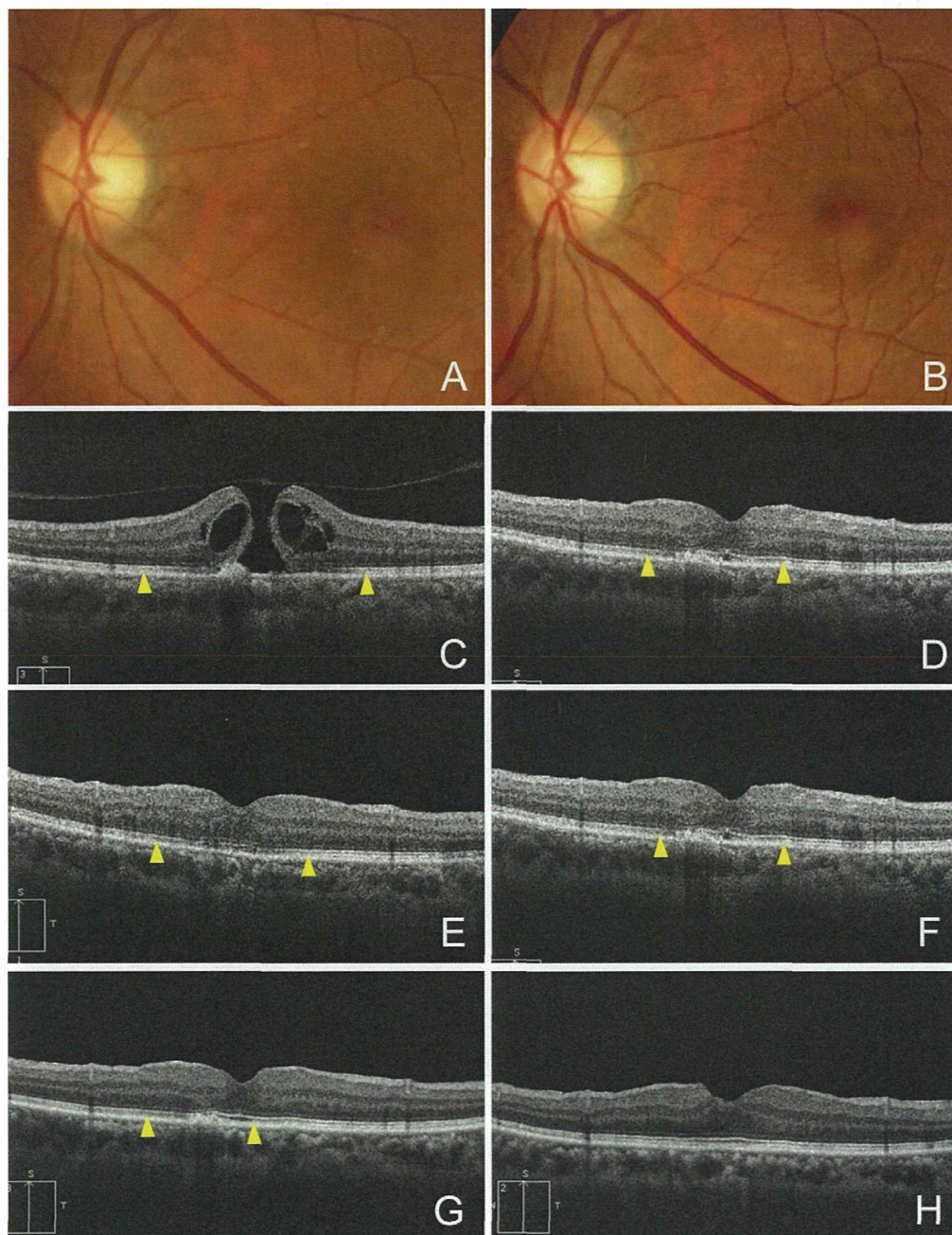


Figure 1. Fundus photograph and spectral domain-optical coherence tomography (SD-OCT) images of eyes with fully recovered cone outer segment tips (COST) line. **A**, Preoperative fundus photograph showing a macular hole. **B**, Postoperative fundus photograph showing a closed macular hole. **C**, Preoperative vertical SD-OCT image of a macular hole with a COST line defect (arrowheads). **D–H**, COST line defect is shorter at 1 month (**D**), 3 months (**E**), 6 months (**F**), and 9 months (**G**) centripetally but not symmetrically at 9 months. **H**, The COST line defect is completely recovered at 12 months.

preoperative stage of the macular hole was stage 2 in 14 eyes (28%), stage 3 in 33 eyes (65%), and stage 4 in 4 eyes (7%).

The mean postoperative decimal BCVA was 0.48 (0.32 logMAR units) at 1 month, 0.61 (0.21 logMAR units) at 3 months, 0.65 (0.19 logMAR units) at 6 months, 0.75 (0.12 logMAR units) at 9 months, and 0.77 (0.11 logMAR units) at 12 months. Each postoperative BCVA was significantly better than the preoperative BCVA ($P < 0.0001$, Student *t* tests).

Spectral-Domain Optical Coherence Tomographic Images of Foveal Microstructures

The correlation between the values obtained by the 2 investigators who measured the length of COST line defect was significant ($r = 0.86$, $P < 0.0001$ preoperatively; $r = 0.91$, $P < 0.0001$ at 1 month postoperatively; $r = 0.89$, $P < 0.0001$ at 3 months postoperatively; $r = 0.90$, $P < 0.0001$ at 6 months postoperatively; $r = 0.89$, $P < 0.0001$ at 9 months postoperatively; and $r = 0.93$, $P < 0.0001$ at 12 months postoperatively; Pearson's correlation coefficient test). The preoperative mean length of the COST line defect was $1666 \pm 474 \mu\text{m}$ (mean \pm standard deviation). The postoperative mean length of COST line defect progressively decreased, and the appearance of the COST line recovery began at the peripheral region and progressed toward the center of the closed macular hole, but not always symmetrically (Figs 1 and 2; Fig 2 available at <http://aoajournal.org>). The mean length was $552 \pm 453 \mu\text{m}$ at 1 month, $407 \pm 356 \mu\text{m}$ at 3 months, $311 \pm 301 \mu\text{m}$ at 6 months, $199 \pm 241 \mu\text{m}$ at 9 months, and $140 \pm 237 \mu\text{m}$ at 12 months (Fig 3). The decrease in the length of the COST line defect was associated with an improvement in the postoperative BCVA. The mean length of the COST line defect at each time was significantly shorter than the preoperative mean length of the COST line defect ($P < 0.0001$, Student *t* tests).

The vertical and horizontal lengths of the COST line defect were not significantly different preoperatively ($P = 0.93$) and at all postoperative times ($P = 0.99$ at 1 month, $P = 0.89$ at 3 months, $P = 0.66$ at 6 months, $P = 0.99$ at 9 months, $P = 0.94$ at 12 months).

Forty-seven eyes were examined 1 month after surgery, and a well-restored IS/OS line and ELM were detected in 8 eyes (17%), an irregular IS/OS line and well-restored ELM were detected in 15 eyes (32%), and an irregular IS/OS line and ELM were detected in 24 eyes (51%). The number of eyes with a well-restored IS/OS line and ELM gradually increased, and the number of eyes with an irregular IS/OS line and ELM gradually decreased during the postoperative period. At 12 months after surgery, a well-restored IS/OS line was detected in 34 (79%) of 43 eyes, and ELM was well restored in all 43 eyes.

Relationship between Length of Cone Outer Segment Tips Line Defect and Visual Acuity

The correlation between the pre- or postoperative BCVA and the length of the COST line defect at each time point was evaluated by simple linear regression analysis. At each postoperative period, the length of the COST line defect was significantly correlated with the BCVA ($P < 0.001$; preoperatively and at 1, 3, 6, 9, and 12 months postoperatively, Fig 4).

Forward stepwise regression analysis was performed to determine whether the postoperative BCVA was correlated with the postoperative length of the COST line, IS/OS junction, and ELM line defect. Our analyses showed that the postoperative BCVA was significantly correlated with the length of COST line defect at 6, 9, and 12 months postoperatively but not at 3 months ($P < 0.001$,

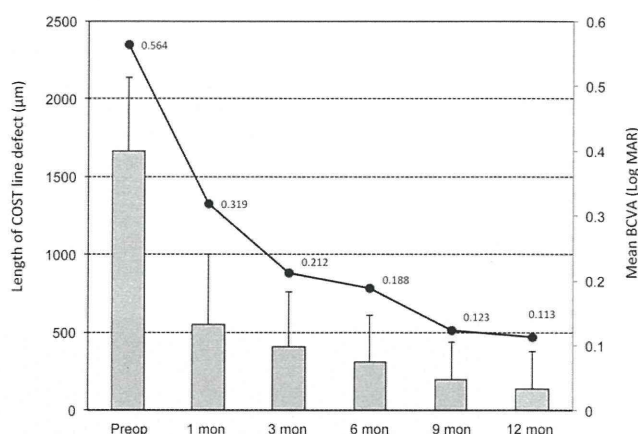


Figure 3. Correlation between visual acuity and mean length of the cone outer segment tips (COST) line defect. The postoperative mean length of the COST line defect gradually decreased. Postoperative best-corrected visual acuity (BCVA) was correlated with the length of COST line defect at the corresponding period. logMAR = logarithm of the minimal angle of resolution.

respectively, Table 2). The postoperative BCVA was correlated with the length of IS/OS junction only at 3 months postoperatively ($P = 0.01$) but not at 6, 9, and 12 months postoperatively ($P = 0.78$, $P = 0.43$, $P = 0.09$, respectively). The postoperative BCVA was not correlated with the length of ELM line defect at 3, 6, and 9 months postoperatively ($P = 0.93$, $P = 0.95$, $P = 0.07$, respectively). The ELM line was completely recovered in all eyes at 12 months postoperatively, and the correlation with postoperative BCVA was not determined. These results indicated that postoperative BCVA was correlated with the length of the IS/OS junction defect at the early postoperative period but not at later times, and the postoperative BCVA was correlated with the COST line defect after 6 months postoperatively.

The correlations between the postoperative BCVA and the preoperative length of the COST line defect, IS/OS junction defect, and ELM line defect were also examined. Forward stepwise regression analysis showed that the preoperative length of COST line defect was significantly correlated with postoperative BCVA at 12 months ($P = 0.02$, Table 3), but not at 3, 6, and 9 months ($P = 0.31$, $P = 0.05$, $P = 0.08$, respectively). The preoperative lengths of the IS/OS junction and ELM line defect were not significantly correlated with the BCVA at 3, 6, 9, and 12 months postoperatively.

Because the preoperative COST line defect was significantly correlated with postoperative vision at 12 months, the correlation of the postoperative BCVA with the length of the COST line defect was determined at each time and evaluated by simple linear regression analysis. Our analyses showed that the preoperative length of the COST line defect was statistically correlated with the BCVA at 1, 3, 6, 9, and 12 months postoperatively ($P < 0.001$ at all times, Fig 5). Thus, the postoperative visual recovery in each time estimated from the preoperative length of COST line defect was significant ($F = 15.4$, $R^2 = 0.35$; $P < 0.001$). The relationship between the preoperative length of the COST line defect and the postoperative BCVA at 12 months is demonstrated by the following equation: $\text{BCVA} = 0.00020 \times L - 0.23$, where the BCVA is the postoperative BCVA in logMAR units at 12 months and L is the preoperative length of the COST line defect in micrometers (95% confidence interval, 0.00010–0.00031).

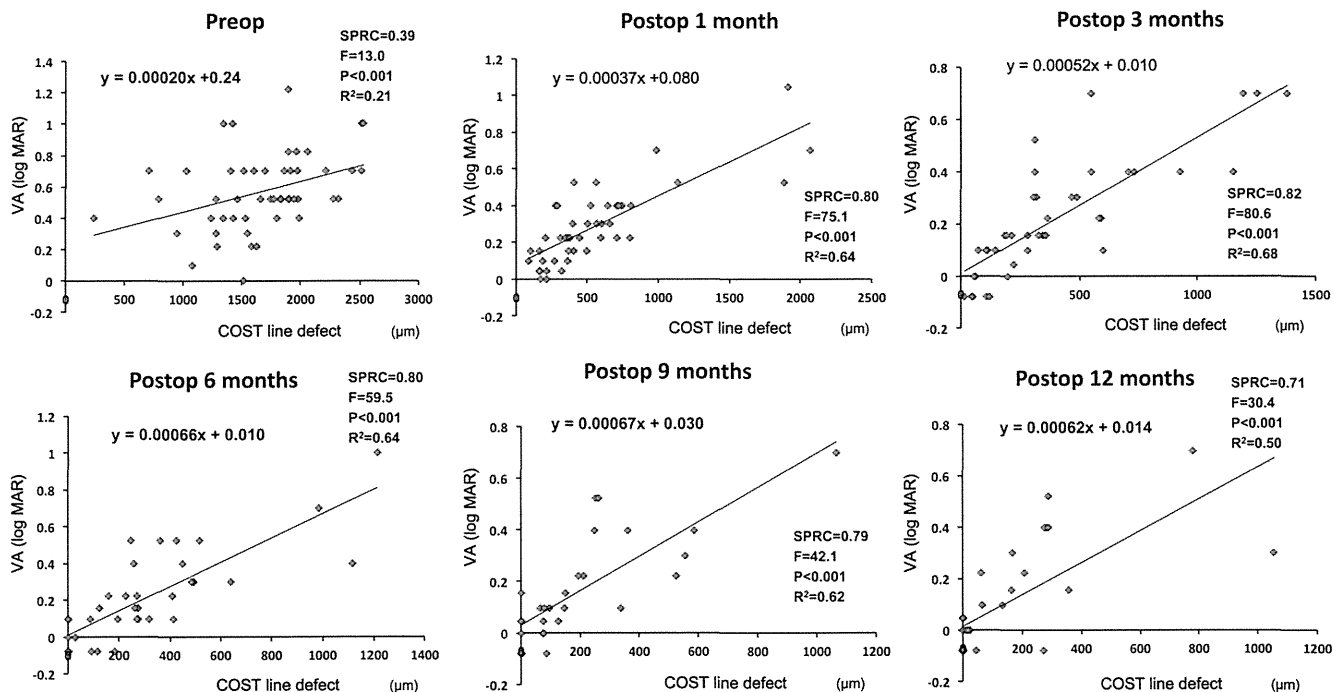


Figure 4. Correlation between length of the cone outer segment tips (COST) line defect and visual acuity at each postoperative time determined by simple linear regression analysis. There are significant correlations between length of the COST line defect and best-corrected visual acuity (BCVA) in the preoperative period and each postoperative period ($P < 0.01$). F = F value; logMAR = logarithm of the minimal angle of resolution; P = P value; Postop = postoperative; Preop = preoperative; R² = coefficient of determination; SPRC = standardized partial regression coefficients; VA = visual acuity.

Relationship between Patients' Demographics and Postoperative Visual Acuity

The demographic factors that were significantly associated with the BCVA at 12 months postoperatively were determined by forward stepwise regression analysis (Table 4). The factors that were found to be significantly associated with postoperative BCVA at 12 months were age ($P = 0.003$) and symptom duration ($P < 0.001$). The gender, preoperative BCVA, axial length, stage of macular hole, preoperative diameter of macular hole, diameter of ILM peeling, and types of gas tamponade during surgery were not significantly associated.

Determination of Preoperative Foveal Microstructure Significantly Associated with Postoperative Best-Corrected Visual Acuity

To determine which preoperative factors were significantly correlated with postoperative BCVA, the lengths of the foveal microstructural line defects and fluid cuff were measured. On the preoperative SD-OCT images of the macular hole, the boundary of the ELM line was seen near the edge of the macular hole even in the elevated sensory retina within the fluid cuff around the macular hole. However, the boundary of IS/OS junction was not visible when the

Table 2. Forward Stepwise Regression Analysis between Spectral-Domain Optical Coherence Tomographic Images and Best-Corrected Visual Acuity at 3, 6, 9, and 12 Months Postoperatively

	3 Mos Postoperatively			6 Mos Postoperatively		
	SPRC	F Value	P Value	SPRC	F Value	P Value
COST line defect	0.022	0.02	0.89	0.74	24.43	<0.001
IS/OS line defect	0.37	7.00	0.01	0.064	0.08	0.78
ELM line defect	0.014	0.01	0.93	0.013	0.003	0.95
	9 Mos Postoperatively			12 Mos Postoperatively*		
	SPRC	F Value	P Value	SPRC	F Value	P Value
COST line defect	0.81	23.57	<0.001	0.62	26.94	<0.001
IS/OS line defect	0.22	0.63	0.43	0.26	3.07	0.09
ELM line defect	-0.46	3.54	0.07	—	—	—

COST = cone outer segment tips; ELM = external limiting membrane; IS/OS = inner segment/outer segment junction; SPRC = standardized partial regression coefficients.

*ELM defect recovered (no defect) at 12 months postoperatively.

Table 3. Forward Stepwise Regression Analysis between Preoperative Spectral-Domain Optical Coherence Tomographic Images and Best-Corrected Visual Acuity at 3, 6, 9, and 12 Months Postoperatively

	3 Mos Postoperatively			6 Mos Postoperatively		
	SPRC	F Value	P Value	SPRC	F Value	P Value
COST line defect	0.19	1.06	0.31	0.35	4.04	0.05
IS/OS line defect	0.38	0.24	0.63	-0.075	0.01	0.92
ELM line defect	-0.08	0.01	0.91	0.32	0.21	0.65

	9 Mos Postoperatively			12 Mos Postoperatively		
	SPRC	F Value	P Value	SPRC	F Value	P Value
COST line defect	0.35	3.30	0.08	0.45	5.81	0.02
IS/OS line defect	0.59	0.54	0.47	0.41	0.27	0.61
ELM line defect	-0.44	0.33	0.57	0.36	0.22	0.64

COST = cone outer segment tips; ELM = external limiting membrane; IS/OS = inner segment/outer segment junction; SPRC = standardized partial regression coefficients.

outer retina was elevated by the fluid cuff (Fig 6). In these eyes, the COST line defect appeared to be larger than the diameter of fluid cuff. The effect of the reduction in the SD-OCT signal by the fluid cuff might be less on the COST line than on the IS/OS junction.

The mean length of the COST line defect ($1666 \pm 474 \mu\text{m}$; mean \pm standard deviation) was significantly longer than the length of the fluid cuff ($761 \pm 243 \mu\text{m}$, $P < 0.01$, 1-way analysis of variance and post hoc Tukey-Kramer test), and the mean length of the ELM line defect ($577 \pm 243 \mu\text{m}$) was significantly shorter than that of the fluid cuff ($P < 0.05$, Fig 7). The mean length of the IS/OS junction defect ($686 \pm 243 \mu\text{m}$) was not significantly differ-

ent from that of the fluid cuff. The mean length of the COST line defect was significantly longer than that of the IS/OS junction and ELM line defects ($P < 0.01$, $P < 0.01$, respectively). The back-reflection of the COST line was reduced in 2 eyes within an elevated outer retina by the fluid cuff around the macular hole.

Discussion

The integrity of the photoreceptor IS/OS line has been reported to be significantly correlated with postoperative

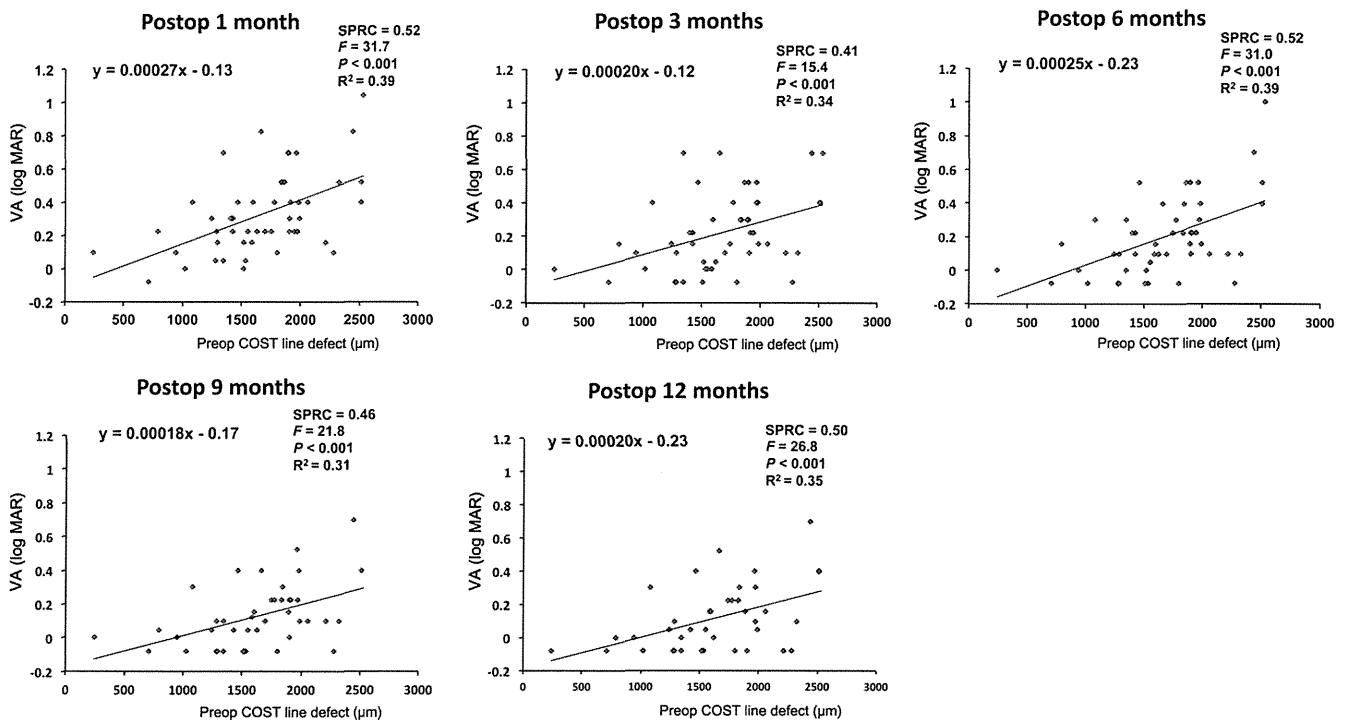


Figure 5. Correlation between preoperative length of cone outer segment tips (COST) line defect and postoperative visual acuity by simple linear regression analysis. There are significant correlations between preoperative length of the COST line defect and best-corrected visual acuity (BCVA) at each postoperative period ($P < 0.001$). logMAR = logarithm of the minimal angle of resolution; R² = coefficient of determination; SPRC = standardized partial regression coefficients; VA = visual acuity.

Table 4. Forward Stepwise Regression Analysis between Patient Baseline Characteristics and Best-Corrected Visual Acuity at 12 Months Postoperatively

	Postoperative BCVA		
	SPRC	F Value	P Value
Age	0.36	9.31	0.004
Gender	0.01	0.01	0.91
Symptom duration	0.53	21.85	<0.001
Axial length	0.09	0.66	0.42
Macular hole diameter	0.17	1.81	0.19
Preoperative BCVA	0.04	0.10	0.75
Stage of macular hole	0.05	0.24	0.63
Diameter of ILM peel	-0.07	0.50	0.48
Types of gas tamponade	0.11	1.11	0.29

BCVA = best-corrected visual acuity; ILM = internal limiting membrane; SPRC = standardized partial regression coefficients.

visual acuity after macular hole surgery.^{5-8,16} The mean total area and maximum length of the IS/OS junction defect at 12 months after surgery were also negatively correlated with the postoperative visual acuity.¹⁰ It is known that the photoreceptors continuously add and shed discs of the outer segments.¹⁹ This renewal of the outer segment has been suggested to be related to the recovery of the length of the foveal photoreceptor outer segments.¹⁹ However, the integrity of the foveal IS/OS junction was not significantly associated with the visual acuity after macular hole surgery because it was not a sign of the photoreceptor cell survival or rearrangement, which is probably more important in determining the visual acuity.¹⁶ This may explain the con-

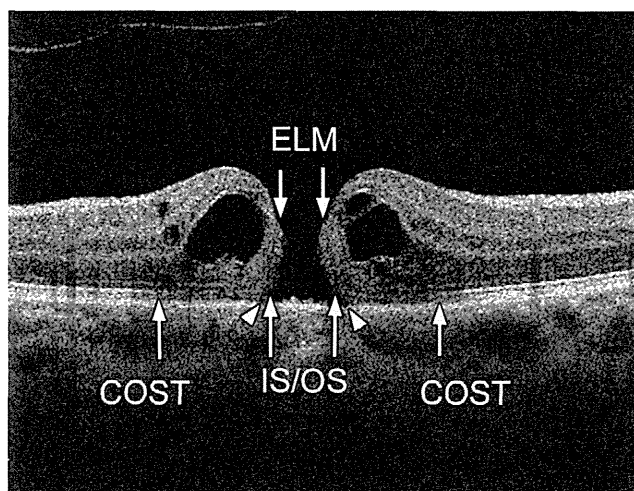


Figure 6. Optical coherence tomographic image of an eye of a 56-year-old woman with a macular hole. The boundaries (white arrows) of the external limiting membrane (ELM) line, inner segment/outer segment (IS/OS) junction, cone outer segment tips (COST) line, and edge of the fluid cuff (white arrowheads) are indicated with decreased signals by the intraretinal cysts. The boundary of the ELM line is seen at the edge of the macular hole, but the boundary of the IS/OS junction is not present beyond the edge of the fluid cuff. The length of the COST line defect is 1904 μm , which is more than the fluid cuff at 576 μm , the ELM line defect at 436 μm , and the IS/OS junction defect at 500 μm .

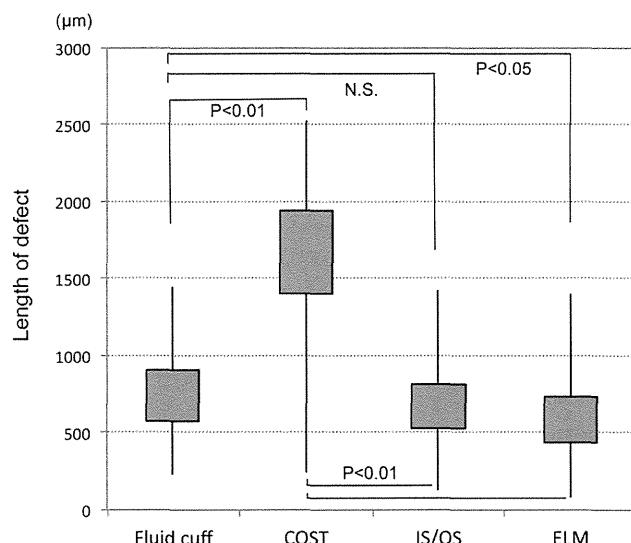


Figure 7. Mean lengths of the foveal microstructural defects at the macular hole. The mean length of the cone outer segment tips (COST) line defect is significantly more than that of the fluid cuff, inner segment/outer segment (IS/OS) junction defect, and external limiting membrane (ELM) line defect. The mean length of the ELM line defect is significantly shorter than that of the fluid cuff. The mean length of the IS/OS junction defect is not significantly different from that of the fluid cuff (1-way analysis of variance and post hoc test of Tukey-Kramer method).

tradictory visual outcomes reported in a recent SD-OCT study.⁶

The integrity of the ELM line, the junction between the inner segment and the Müller cells, was reported to be another important morphologic structure of the photoreceptor microstructure that was related to the visual acuity in patients after macular hole closure¹⁴⁻¹⁶ and macula retinal reattachment.^{20,21} A continuous ELM has been considered to be a sign of intact photoreceptor cell bodies and Müller cells, and the IS/OS junction rarely recovered without a recovery of the ELM.^{14,16,18,22} However, our results suggested that postoperative visual acuity was more highly correlated with the length of the COST line defect rather than the length of the IS/OS and ELM line defects.

We recently reported a significant correlation between the visual acuity and the integrity of foveal COST line after successful macular hole surgery.¹⁸ The recovered COST line was observed only in eyes with an intact IS/OS junction and ELM. The eyes with visual acuity $\geq 20/25$ at 12 months postoperatively were more frequently associated with the eyes that had a recovered COST line because the recovered cones were functioning normally.¹⁸ In this study, we found that the length of the COST line defect was significantly correlated with visual acuity at each postoperative period. However, the lengths of the IS/OS junction and ELM line defect were not significantly correlated with visual acuity 6 months postoperatively, indicating that the recovery of the COST line was more important for postoperative visual acuity than the recovery of the IS/OS junction and ELM line. Chang et al⁶ suggested that the length of the IS/OS junction was not correlated with visual acuity after macular hole surgery because the IS/OS defect occurred in edema-

tous retinal areas. Oh et al¹¹ reported that the shape of IS/OS junction defect area was round and regular before macular hole surgery but turned irregular after surgery. They found that the postoperative area of the IS/OS defect was more strongly correlated with the BCVA than the length of the defect measured by linear-based raster scans because of the irregular shape of the IS/OS defect area after surgery.¹¹

Reconstruction of the foveal ELM line in the early postoperative period can help to predict subsequent restoration of the foveal photoreceptor layer and the potential for better visual outcomes.^{16,20} Ooka et al¹⁴ reported that the preoperative IS/OS or ELM line defect was significantly associated with the postoperative foveal sensitivity detected by MP1 microperimetry but not significantly associated with the postoperative BCVA. Thus, they estimated the postoperative sensitivity at 6 months from the preoperative length of the IS/OS junction and ELM line defects, but the postoperative BCVA could not be predicted.¹⁴ We found that the preoperative length of the COST line defect was significantly correlated with postoperative visual acuity at 12 months, but the preoperative length of the IS/OS junction and ELM line defects were not.

On the preoperative SD-OCT image, the edge of a macular hole was elevated with a surrounding cuff of subretinal fluid. Within the elevated outer retina around the macular hole, the back-reflection of the IS/OS line was reduced, whereas the visibility of the ELM line was retained.^{4,14} Hangai et al⁴ reported that the ELM back-reflecting line could be used to delineate the photoreceptor inner and outer segment reflectivity within the elevated outer retina around the macular hole. However, the length of the ELM line defect is affected by the height of the elevated retina around the macular hole. Consequently, an evaluation of both the IS/OS junction and the ELM line may not accurately indicate the status of the preoperative foveal photoreceptor microstructures in patients with macular hole.

We found that the length of the COST line defect was greater than the length of the IS/OS junction defect, the ELM defect, and the diameter of fluid cuff in the preoperative SD-OCT images. We have not evaluated the effect of the fluid cuff on the SD-OCT signals of the COST line around the macular hole. However, we assume that when the preoperative factor to predict postoperative visual recovery in SD-OCT findings was considered, the COST line defect had an advantage because it was minimally affected by the fluid cuff as a result of the significantly larger COST line defect compared with the fluid cuff. In our cases, the back-reflection of the COST line was diminished in 2 eyes within the elevated outer retina by a fluid cuff around the macular hole. Further development of retinal imaging and further studies with a larger sample size are needed to clarify this issue.

This study was a retrospective study without a control group. Also, the number of patients in each group was small, and the resolution of conventional SD-OCT used in the study was limited to detect the COST line compared with the ultra-high-resolution OCT. However, we have found that an intact foveal COST line could be detected in 95% of healthy normal eyes with conventional SD-OCT.²³ Therefore, further studies with a larger sample size and

higher-resolution SD-OCT are needed to confirm these results, including the asymmetric recovery of the COST line defect. Nevertheless, the results showed that the integrity of the COST line rather than from the IS/OS junction and ELM lines may be more clinically useful to indicate postoperative visual recovery in patients with surgically closed macular holes.

Symptom duration was a preoperative factor that was significantly correlated with postoperative vision. However, symptom duration may not always be reliable when patients are unaware of the unilateral visual deterioration.²⁴ We assumed that measurement of the preoperative length of the COST line may be a more objective factor to predict postoperative visual recovery.

In conclusion, our quantitative measurements of the photoreceptor COST line defects showed that the recovery of the photoreceptor COST line was correlated with the BCVA after macular hole surgery. In addition, the preoperative COST line defect may be able to predict visual acuity after successful macular hole closure.

References

1. Wolf S, Wolf-Schnurrbusch U. Spectral-domain optical coherence tomography use in macular diseases: a review. *Ophthalmologica* 2010;224:333–40.
2. Koizumi H, Spaide RF, Fisher YL, et al. Three-dimensional evaluation of vitreomacular traction and epiretinal membrane using spectral-domain optical coherence tomography. *Am J Ophthalmol* 2008;145:509–17.
3. Chang LK, Fine HF, Spaide RF, et al. Ultrastructural correlation of spectral-domain optical coherence tomographic findings in vitreomacular traction syndrome. *Am J Ophthalmol* 2008;146:121–7.
4. Hangai M, Ojima Y, Gotoh N, et al. Three-dimensional imaging of macular holes with high-speed optical coherence tomography. *Ophthalmology* 2007;114:763–73.
5. Baba T, Yamamoto S, Arai M, et al. Correlation of visual recovery and presence of photoreceptor inner/outer segment junction in optical coherence images after successful macular hole repair. *Retina* 2008;28:453–8.
6. Chang LK, Koizumi H, Spaide RF. Disruption of the photoreceptor inner segment-outer segment junction in eyes with macular holes. *Retina* 2008;28:969–75.
7. Lee JE, Lee SU, Jea SY, et al. Reorganization of photoreceptor layer on optical coherence tomography concurrent with visual improvement after macular hole surgery. *Korean J Ophthalmol* 2008;22:137–42.
8. Haritoglou C, Neubauer AS, Reiniger IW, et al. Long-term functional outcome of macular hole surgery correlated to optical coherence tomography measurements. *Clin Experiment Ophthalmol* 2007;35:208–13.
9. Christensen UC, Krøyer K, Sander B, et al. Prognostic significance of delayed structural recovery after macular hole surgery. *Ophthalmology* 2009;116:2430–6.
10. Inoue M, Watanabe Y, Arakawa A, et al. Spectral-domain optical coherence tomography images of inner/outer segment junctions and macular hole surgery outcomes. *Graefes Arch Clin Exp Ophthalmol* 2009;247:325–30.
11. Oh J, Smiddy WE, Flynn HW Jr, et al. Photoreceptor inner/outer segment defect imaging by spectral domain OCT and visual prognosis after macular hole surgery. *Invest Ophthalmol Vis Sci* 2010;51:1651–8.

12. Sano M, Shimoda Y, Hashimoto H, Kishi S. Restored photoreceptor outer segment and visual recovery after macular hole closure. *Am J Ophthalmol* 2009;147:313–8.
13. Michalewska Z, Michalewski J, Cisiecki S, et al. Correlation between foveal structure and visual outcome following macular hole surgery: a spectral optical coherence tomography study. *Graefes Arch Clin Exp Ophthalmol* 2008;246:823–30.
14. Ooka E, Mitamura Y, Baba T, et al. Foveal microstructure on spectral-domain optical coherence tomographic images and visual function after macular hole surgery. *Am J Ophthalmol* 2011;152:283–90.
15. Shimozone M, Oishi A, Hata M, Kurimoto Y. Restoration of the photoreceptor outer segment and visual outcomes after macular hole closure: spectral-domain optical coherence tomography analysis. *Graefes Arch Clin Exp Ophthalmol* 2011;249:1469–76.
16. Wakabayashi T, Fujiwara M, Sakaguchi H, et al. Foveal microstructure and visual acuity in surgically closed macular holes: spectral-domain optical coherence tomographic analysis. *Ophthalmology* 2010;117:1815–24.
17. Srinivasan VJ, Monson BK, Wojtkowski M, et al. Characterization of outer retinal morphology with high-speed, ultrahigh-resolution optical coherence tomography. *Invest Ophthalmol Vis Sci* 2008;49:1571–9.
18. Itoh Y, Inoue M, Rii T, et al. Significant correlation between visual acuity and recovery of foveal cone microstructures after macular hole surgery. *Am J Ophthalmol* 2012;153:111–9.
19. Guérin CJ, Lewis GP, Fisher SK, Anderson DH. Recovery of photoreceptor outer segment length and analysis of membrane assembly rates in regenerating primate photoreceptor outer segments. *Invest Ophthalmol Vis Sci* 1993;34:175–83.
20. Wakabayashi T, Oshima Y, Fujimoto H, et al. Foveal microstructure and visual acuity after retinal detachment repair: imaging analysis by Fourier-domain optical coherence tomography. *Ophthalmology* 2009;116:519–28.
21. Shimoda Y, Sano M, Hashimoto H, et al. Restoration of photoreceptor outer segment after vitrectomy for retinal detachment. *Am J Ophthalmol* 2010;149:284–90.
22. Bottoni F, De Angelis S, Luccarelli S, et al. The dynamic healing process of idiopathic macular holes after surgical repair: a spectral-domain optical coherence tomography study. *Invest Ophthalmol Vis Sci* 2011;52:4439–46.
23. Rii T, Itoh Y, Inoue M, Hirakata A. Foveal cone outer segment tips line and disruption artifacts in spectral domain optical coherence tomographic images of normal eyes. *Am J Ophthalmol* 2012;153:524–9.
24. Ullrich S, Haritoglou C, Gass C, et al. Macular hole size as a prognostic factor in macular hole surgery. *Br J Ophthalmol* 2002;86:390–3.

Footnotes and Financial Disclosures

Originally received: August 14, 2011.

Final revision: January 11, 2012.

Accepted: January 12, 2012.

Available online: March 14, 2012. Manuscript no. 2011-1225.

Kyorin Eye Center, Kyorin University School of Medicine, Tokyo, Japan.

Presented at: the American Academy of Ophthalmology annual meeting, October 22-25, 2011, Orlando, Florida.

Financial Disclosure(s):

The authors indicate no government or nongovernment financial support was involved in the work for this submission. Dr. Inoue has received

speaker support from Alcon Japan, Ltd., Santen Pharmaceutical Inc., HOYA Corp, and Kowa Pharmaceutical Co. Ltd. Dr. Hirakata has received speaker support from Alcon Japan, Ltd., Santen Pharmaceutical Inc., Novartis Pharma K.K., and Senju Pharmaceutical Co., Ltd. The other authors declare that they have no financial interest.

This article contains online-only material. Figure 2 should appear online-only.

Correspondence:

Makoto Inoue, MD, Kyorin Eye Center, Kyorin University School of Medicine, 6-20-2 Shinkawa, Mitaka, Tokyo, 181-8611, Japan. E-mail: inoue@eye-center.org.

Intrachoroidal Cavitation in Macular Area of Eyes With Pathologic Myopia

KYOKO OHNO-MATSUI, MASAHIRO AKIBA, MUKA MORIYAMA, TATSURO ISHIBASHI, AKITO HIRAKATA, AND TAKASHI TOKORO

- **PURPOSE:** To determine the incidence and characteristics of intrachoroidal cavitations in the macular area of eyes with high myopia.
- **DESIGN:** Prospective, noninterventional case series.
- **METHODS:** We evaluated 56 eyes of 44 patients with pathologic myopia (myopic spherical equivalent >8 diopters) and with patchy chorioretinal atrophy using a swept-source optical coherence tomographic (OCT) system with a center wavelength of 1050 nm. We focused on the changes in the scleral curvature in the area of patchy atrophy. The relationship of the macular intrachoroidal cavitation and retinoschisis was also analyzed. Sixty-eight consecutive patients with pathologic myopia but without patchy atrophy were analyzed as controls.
- **RESULTS:** In 31 of 56 eyes (55.4%) with patchy atrophy, the swept-source OCT images showed that the sclera was bowed posteriorly in and around the patchy atrophy compared to neighboring sclera, whereas none of the 68 patients without patchy atrophy showed this finding. Macular intrachoroidal cavitation had OCT features similar to peripapillary intrachoroidal cavitation; the choroid in the macular intrachoroidal cavitation area appeared thickened and the retina was caved into the cavitation. There was a direct communication between the vitreous and intrachoroidal cavitation in 3 eyes. Retinoschisis was observed significantly more frequently in or around the patchy atrophy in eyes with macular intrachoroidal cavitation than in those without cavitation.
- **CONCLUSIONS:** These findings suggest that patchy atrophy affects the scleral contour within posterior staphyloma beyond the funduscopically identified patchy atrophy by macular intrachoroidal cavitation. Such deformation of sclera may facilitate the development of retinoschisis in and around the patchy atrophy. (Am J Ophthalmol 2012;154:382–393. © 2012 by Elsevier Inc. All rights reserved.)

PATHOLOGIC MYOPIA IS A MAJOR CAUSE OF VISUAL impairment worldwide.^{1–6} The visual impairment is mainly attributable to the development of myopic macular lesions secondary to the excessive increase of the axial length of the eyes and the development of posterior staphylomas.^{7–9} The myopic macular lesions include myopic choroidal neovascularization (CNV), myopic macular retinoschisis, and myopic chorioretinal atrophy. The myopic chorioretinal atrophies are classified into 2 types based on the fundus findings: diffuse chorioretinal atrophy and patchy chorioretinal atrophy.⁸ A diffuse chorioretinal atrophy is an ill-defined yellowish-white atrophy and the vision is not severely affected. A patchy chorioretinal atrophy, on the other hand, is a grayish-white lesion with well-defined borders. This appearance is believed to be caused by a complete loss of the choriocapillaris⁸ and the subsequent degeneration of the photoreceptors and the retinal pigment epithelium (RPE) because of the loss of the choriocapillaris. This area of patchy atrophy is associated with an absolute scotoma. An enlargement of a patchy chorioretinal atrophy is the main cause of central vision loss in patients with pathologic myopia.⁸ The morphology of a patchy chorioretinal atrophy has been studied by conventional ophthalmoscopy.¹⁰

Spectral-domain optical coherence tomography (OCT) has also been used to study patchy chorioretinal atrophies. However, these instruments are limited to what can be observed at the surface of the tissue. It has not been possible to observe the morphologic structure of the deeper tissues such as the sclera in the area of the patchy atrophy by these conventional methods. Swept-source OCT uses a wavelength-sweeping laser as the light source,¹¹ and in practice, it has less sensitivity roll-off with tissue depth than conventional spectral-domain OCTs. The current swept-source OCT instruments use a longer center wavelength, generally in the 1-micrometer range, which has improved their ability to penetrate deeper into tissues than the conventional spectral-domain OCT instruments. With the ability of imaging deeper structures in the eye, evaluations of their morphology, such as that of the entire layer of choroid¹² and retrobulbar part of the optic nerve,^{13,14} are potentially possible.

When we examined highly myopic patients with a swept-source OCT, we noticed that the sclera was bowed posteriorly in the area of the patchy atrophy in many of these eyes. This area then resembled the intrachoroidal

Accepted for publication Feb 3, 2012.

From the Department of Ophthalmology and Visual Science, Tokyo Medical and Dental University, Tokyo, Japan (K.O.M., M.M., T.T.); Topcon Corporation, Tokyo, Japan (M.A.); Department of Ophthalmology, Kyushu University, Fukuoka, Japan (T.I.); and Department of Ophthalmology, Kyorin University School of Medicine, Tokyo, Japan (A.H.).

Inquiries to Kyoko Ohno-Matsui, Dept of Ophthalmology and Visual Science, Tokyo Medical and Dental University, 1-5-45 Yushima, Bunkyo-ku, Tokyo 113, Japan; e-mail: k.ohno.oph@tmd.ac.jp